Int. J. Electrochem. Sci., 14 **(2019)** 9221 – 9230, doi: 10.20964/2019.09.63

International Journal of
ELECTROCHEMICAL
SCIENCE
www.electrochemsci.org

Short Communication

Study of the Hydrogen Delayed Fracture of Mooring Chain Steel using Strain Rate Testing

Songjie Li[1], *Panfei Sun*[1], *Jiang Yin*[2], *Maoqiu Wang*[3], *Chengduo Wang*[4,*], *Lixiang Shao*[1], *Fan Li*[1], *Yuanyuan Li*[1]

[1] School of Chemical Engineering and Energy, Zhengzhou University, Zhengzhou 450001, P. R. China
[2] Asian Star Anchor Chain Co., Ltd., Jingjiang 214533, P. R. China
[3] Institute for Special Steels, Central Iron and Steel Research Institute, Beijing 100081, P. R. China
[4] School of Material Science and Engineering, Zhengzhou University, Zhengzhou 450001, P. R. China
[*]E-mail: wangchengduo@163.com

Received: 5 May 2019 / *Accepted:* 18 June 2019 / *Published:* 5 August 2019

The delayed fracture behaviour of a high-strength offshore mooring chain steel was investigated by a conventional strain rate test (CSRT). The hydrogen was electrochemically pre-introduced to the steel, and the hydrogen content in the specimen was measured by thermal desorption analysis (TDA) after fracturing during the CSRT. The results showed that when the hydrogen content was less than 3.0 wppm, the fracture stress decreased slowly and linearly. As the hydrogen content exceeded 3.0 wppm, the fracture stress decreased rapidly but remained linear. With increasing of hydrogen content the fracture mode changed from ductile to brittle intergranular. The dependence of local maximum fracture stress on local hydrogen content obtained from the CSRT and slow strain rate test (SSRT) was similar when the local hydrogen content was less than 3.0 wppm. However, when the hydrogen content was more than 3.0 wppm, at a given nominal fracture stress, the local hydrogen content for the CSRT was lower than that for the SSRT.

Keywords: hydrogen delayed fracture; offshore mooring chain steel; thermal desorption analysis; diffusible hydrogen content; conventional strain rate test

1. INTRODUCTION

Recently, a substantial amount of attention is being given to the extraction of energy resources from the deep sea as the demand for oil and gas increases. To ensure the safety of offshore floating installations, a mooring system is indispensable. As the main material used for offshore mooring, chain steel with high strength and good corrosion resistance should be developed for severe marine environments. Furthermore, to exploit reserves in deep oceans, a longer mooring chain is required, and

the corresponding added weight requires a chain steel with increased strength. However, it is known that high-strength steel is susceptible to hydrogen with increasing strength, which is generally referred to as delayed fracture or hydrogen embrittlement [1–5].

Due to working in a severely corrosive environment, mooring chain steel with a tensile strength over 690 MPa is generally regarded as a high-strength steel. Hydrogen could be introduced into the chain steel as a by-product of marine corrosion or by the inappropriate operation of cathodic protection systems [6–11]. In the past, many studies have been performed on hydrogen-delayed fracture of high-strength steels [12–20]. However, hydrogen-delayed fracture has seldom been studied for high-strength mooring chain steels, although they are increasingly used in deep-sea environments. This seriously affects the safe engineering design of mooring systems.

The critical diffusible hydrogen content (H_C) is regarded as one of the important factors that causes fracture [12, 21, 22]. The dependence of the fracture stress on critical diffusible hydrogen content introduced by electrochemical hydrogen charging has been previously studied with a slow strain rate test (SSRT) [23–25], constant loading test (CLT) [26, 27], and conventional strain rate test (CSRT) [28–31], to name a few. After these tests, the corresponding hydrogen content is measured by thermal desorption analysis (TDA). Each CLT and SSRT, takes several hours, and the specimen is usually electroplated with cadmium to prevent hydrogen release. However, a CSRT takes 1-5 minutes at a conventional speed, and thus, the hydrogen diffusion could be neglected. The specimen does not need to be coated during test and many specimens could be tested quickly. In this study, the delayed fracture behaviour of mooring chain steel was investigated with a CSRT combined with TDA using electrochemical hydrogen pre-charged notched bar specimens.

2. EXPERIMENTAL PROCEDURES

2.1 Materials and CSRT

Mooring chain steel with a tensile strength of 1200 MPa was used in this study. The nominal composition was 0.22 C-0.25 Si-0.30 Mn-0.15 (V+Nb+Ti)-4.9 (Cr+Ni+Mo) (wt%). As shown in Fig. 1, a circumferentially notched round bar specimen was used for the CSRT with a calculated stress concentration factor of 4.9 [32].

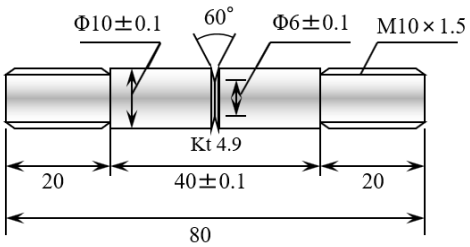

Figure 1. Dimensions (in mm) of the notched specimen for the CSRT with a notch root radius of 0.1 mm.

The hydrogen was electrochemically pre-charged into the CSRT specimens in a 0.1 mol/L NaOH solution or a H_2SO_4 solution at a current density from 1 A/m^2 to 10 A/m^2 for 96 h [33]. Then, the CSRT was carried out on a WDML-300 kN tensile testing machine with a constant crosshead speed of 1 mm/min. As soon as the specimens fractured, they were immediately stored in liquid nitrogen until the hydrogen content was measured. The nominal fracture stress, σ_f, was calculated with equation (1):

$$\sigma_f = F_{max}/A_{min} \quad (1)$$

where F_{max} is the maximum tensile load, A_{min} is the initial cross-section area around the notch.

2.2 TDA measurement

The hydrogen content was measured by TDA with an instrument developed by R-Dec Co. Ltd. combined with the National Institute for Materials Science (NIMS). The accuracy of the hydrogen content reached 0.01 wppm (wt%). TDA measurement was conducted from room temperature to 1073 K at a heating rate of 100 K/h. The hydrogen diffusion content (H_D) in the specimen is important for delayed fracture, as reported by Takai and Watanuki [13].

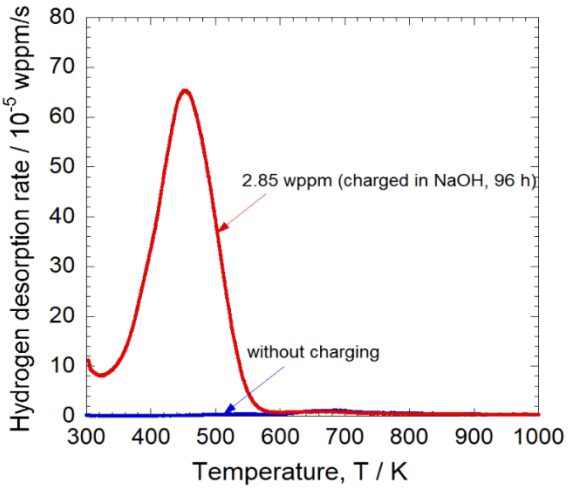

Figure 2. TDA curves of the mooring chain steel for with and without hydrogen charging in a 0.1 mol/L NaOH solution with a current density of 1 A/m^2 for 96 h.

The typical hydrogen desorption curves for the specimens with and without hydrogen charging are shown in Fig. 2. There is an obvious desorption peak of hydrogen at approximately 450 K for the hydrogen charged specimen, while no peak appears for without charging. As reported in a previous study [23, 34], according to the dependence of peak temperatures on the heating rates, the activation energy (Ea) of hydrogen desorption could be calculated with equation (2):

$$\frac{\partial \ln(\frac{\emptyset}{T_c^2})}{\partial(\frac{1}{T_c})} = -\frac{E_a}{R} \quad (2)$$

where Φ is the heating rate, T_c is the peak temperature.

2.3 Microscopic observations

The polished steel specimen etched with a Nital solution (2% HNO_3 in alcohol) was observed with a METAVAL optical microscope to study the microstructure. The fracture surface after CSRT was observed with scanning electron microscopy (SEM) on a JSM 7500F operating at 15 kV. In particular, the fractured specimen with diffusible hydrogen content of 3.22 wppm was sectioned and polished to obtain a damage-free surface, and its microcracks were examined by electron backscatter diffraction (EBSD) in a Zeiss LEO 1550 SEM. A step size of 0.15 μm was used in the EBSD scans. The data were obtained using the grain dilation provided by the TexSEM Laboratories (TSL) software.

3. RESULTS AND DISCUSSION

The microstructure of the high-strength mooring chain steel used is shown in Fig. 3. The grain size of the specimen was approximately 10 μm, and a microstructure of tempered sorbite was indicated by the uniformly dispersed fine carbide precipitates in the matrix.

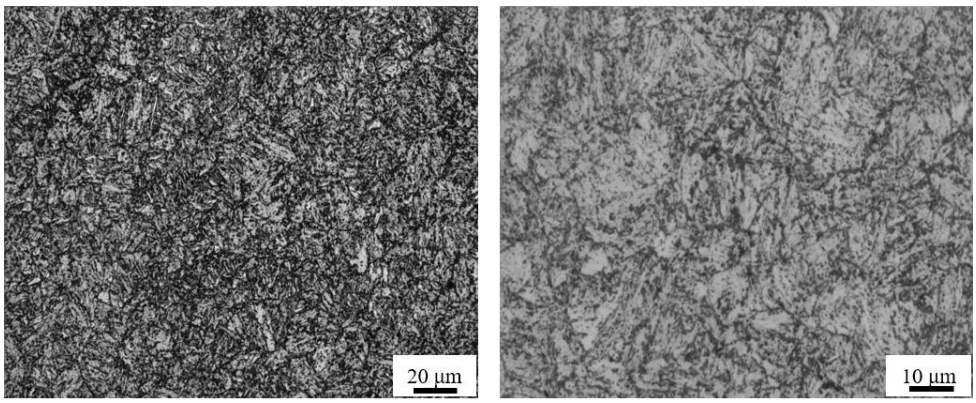

Figure 3. Microstructure of high-strength mooring chain stain used in this study.

Typical TDA curves for the specimens charged in the NaOH solution and fractured by the CSRT are shown in Fig. 4. In this study, the highest hydrogen content reached 9.0 wppm and was obtained by charging in the H_2SO_4 solution. There was no obvious hydrogen desorption peak for uncharged specimen. For the charged specimens, additional hydrogen desorption peaks appeared at approximately 420 K-450 K, and were regarded as diffusible hydrogen.

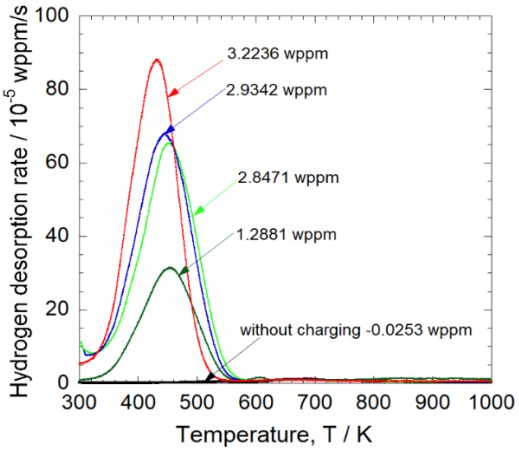

Figure 4. TDA curves of notched specimens for without hydrogen charging and with hydrogen pre-charged in a 0.1 mol/L NaOH solution with different charge densities (1-10 A/m^2) measured after CSRT.

Basing on the plot of ln(Φ/Tc^2) against (1/Tc) for the desorption peak corresponding to diffusible hydrogen shown in Figure 5, the activation energy (Ea) of hydrogen desorption was calculated to be 18.6 kJ/mol from the slope of the linear regression line according to equation (2). Based on a previous study, the measured diffusible hydrogen for the mooring chain steel was probably trapped by grain boundaries and dislocations [22, 23, 35].

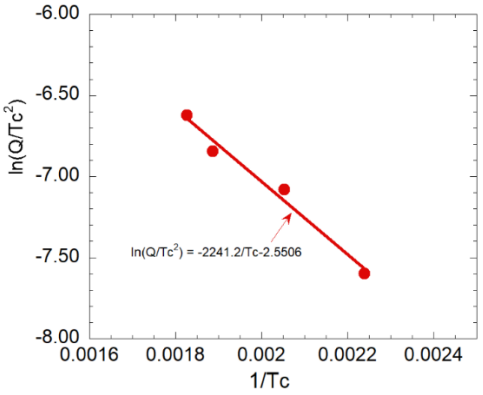

Figure 5. Activation energy (Ea) of hydrogen desorption obtained by plots of ln (Φ/Tc^2) against 1/Tc, where Φ is the heating rate, T_c is the peak temperature.

The dependence of fracture stress on hydrogen content obtained by the CSRT is shown in Fig. 6. For comparison, the results from our previous SSRT [33] were also plotted in the figure. In the two cases, the decrease in the fracture stresses had an obvious inflection point with increasing diffusible hydrogen content. For the CSRT, the fracture stress decreased linearly and slowly with increasing diffusible hydrogen content when it was less than 3.0 wppm. As the hydrogen content exceeded 3.0

wppm, the fracture stress decreased rapidly but remained linear while for the SSRT, the rapid decrease in the fracture stress was not linear.

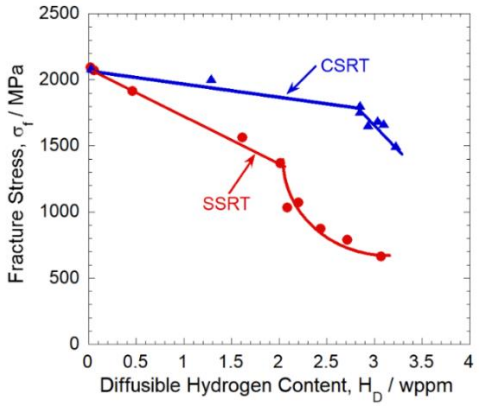

Figure 6. Dependence of the fracture stress on diffusible hydrogen content for CSRTed and SSRTed mooring chain steel specimens.

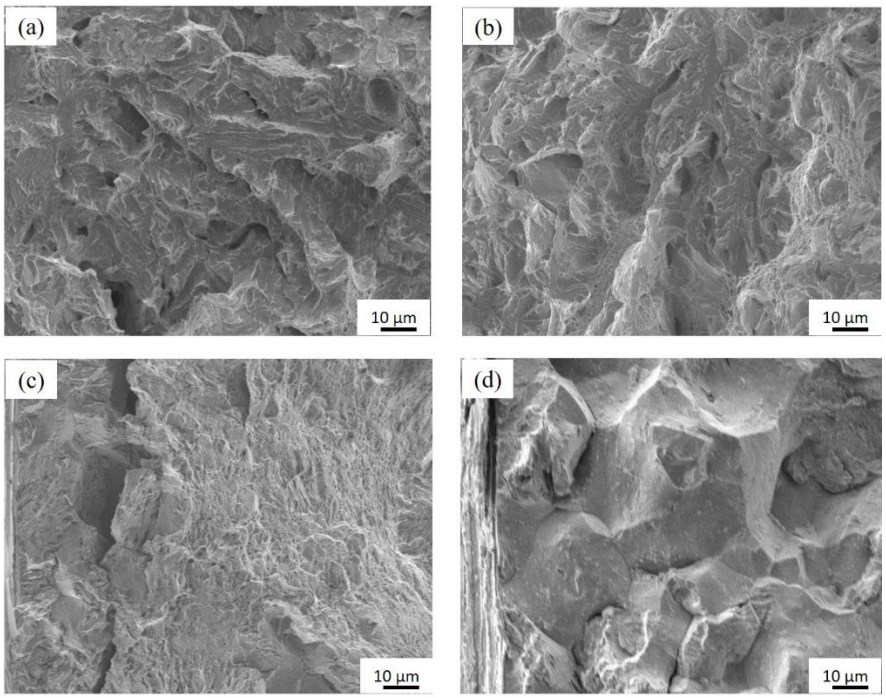

Figure 7. SEM images of mooring chain steel specimens with diffusible hydrogen content: (a) H_D = 0.02 wppm, (b) H_D = 2.85 wppm, (c) H_D = 3.22 wppm, and (d) H_D = 9.0 wppm.

Figure 7 shows the fracture surface at the crack initiation site for the uncharged and charged specimens with different diffusible hydrogen contents. The specimen with a diffusible hydrogen content of 2.85 wppm (Fig. 7b) exhibited a ductile fracture mode, which is the same mode as the uncharged specimen (Fig. 7a). However, as the diffusible hydrogen content increased to 3.22 wppm (Fig. 7c), intergranular fracture appeared for the charged specimen. Furthermore, when the hydrogen content reached 9.0 wppm (Fig. 7d), the fracture mode of the charged specimen was brittle intergranular fracture.

It can be assumed that the ratio of intergranular fracture increased with hydrogen content. Figure 8 shows the inverse pole figure (IPF) map combined with image quality (IQ) around cracks in the specimens with a diffusible hydrogen content of 3.22 wppm.

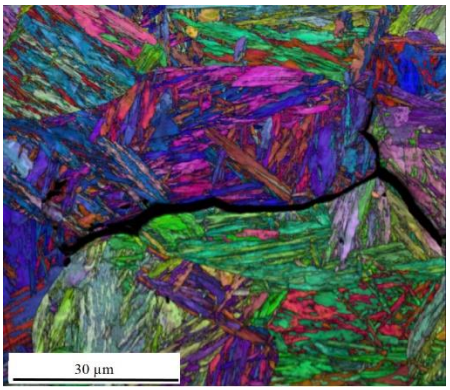

Figure 8. The inverse pole figure (IPF) map combined with image quality (IQ) around cracks in the specimens with a diffusible hydrogen content of 3.22 wppm.

Clearly, the orientations on both sides of the cracks were different. This means that the cracks originated from the grain boundaries. This result supports the fact that intergranular fracture appeard in the charged specimens with a hydrogen content of 3.22 wppm. Furthermore, we identified they are austenite grain boundaries using the method of Wang [36].

It was reported by Wang and Hagihara et al [23, 37] that the relationship between the local diffusible hydrogen content (H*) and the maximum local stress (σ_m) for the CSRT and SSRT at the initiation site was almost the same for steels with strengths of 1300-1500 MPa. To compare the results obtained from the CSRT and SSRT, the local maximum fracture stress (σ_m) and the local diffusible hydrogen content (H*) were calculated. The local maximum fracture stress was calculated based on a previous study of a notched specimen with a Kt of 4.9 [38]. The local content of hydrogen at the crack initiation site for the CSRT was equal to the measured hydrogen content H_D. For the SSRT, the local diffusible hydrogen content accumulated by stress-induced diffusion can be calculated by equation (3) [23, 38].

$$H^* = H_D \exp\left[\frac{-V_H(\sigma_h - \sigma_{h,min})}{RT}\right] \quad (3)$$

where H* is the local hydrogen content, H_D is the diffusible hydrogen content measured by the TDA for SSRTed specimen; σ_h is the hydrostatic stress at the stress concentration region; $\sigma_{h,\,min}$ is the hydrostatic stress in the region far from the notched section, V_H equals 2.1×10^{-6} m^3/mol [39], R is the gas constant and T is 300 K.

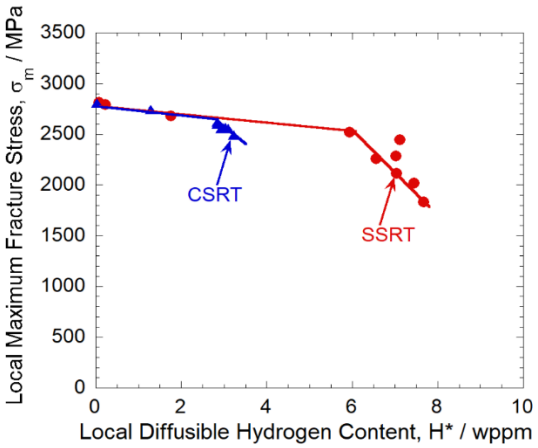

Figure 9. Dependence of local maximum fracture stress on local diffusible hydrogen content for CSRTed and SSRTed mooring chain steel specimens.

The relationship between the local maximum fracture stress and local hydrogen content for CSRTed and SSRTed specimens is shown in Fig. 9. We can see that when H* was less than 3.0 wppm the relationship between σ_m and H* for the CSRTed specimen was the same as that for the SSRTed specimen. However, the local hydrogen content of over 3.0 wppm for the CSRTed specimen was lower than that of SSRTed specimen at a given nominal fracture stress. This result differs from that of a previous study reported by Hagihara et al [28–30]. One possible reason is the difference in the strength level. Our mooring strain steel in this study had a tensile strenght of 1200 Mpa, while steels with 1300 MPa and 1500 MPa grade tensile strengths were used by Hagihara et al. Another reason is probably the effect of VC precipitation, which can affect several parameters in equation (3) being similar with that reported by Chida et al [37].

4. SUMMARY

The delayed fracture behaviour of high-strength mooring chain steel with a tensile strength 1200 MPa was evaluated by the conventional strain rate test (CSRT), and the electrochemically charged hydrogen content was measured by thermal desorption analysis (TDA). The results show that the fracture stress decreased linearly with increasing diffusible hydrogen content. However, the rate of decrease grew as the hydrogen content reached approximately 3.0 wppm, corresponding to the fracture mode changing from ductile to intergranular. The calculated results of the local maximum fracture stress and local hydrogen content show that the relationship between σ_m and H* from the CSRT and SSRT were the same when the local hydrogen content was less than 3.0 wppm. However, the local hydrogen content for the CSRT was lower than that for the SSRT at a given nominal fracture stress for more than 3.0 wppm, which is different from the previous study.

ACKNOWLEDGMENTS
This work is partially supported by a grant from the National Natural Science Foundation of China (Grant no. 51601170), Scientific and Technological Project of Henan Province (No. 182102210012) and CSC Scholarship (No. 201807045063). These grants are gratefully acknowledged.

References

1. H.C. Rogers, *Science*, 159 (1968) 1057.
2. J.P. Hirth, *Metall. Trans. A*, 11 (1980) 861.
3. W. Chu, J. Yao and C. Hsiao, *Metall. Trans. A*, 15 (1984) 729.
4. M. Nagumo, *ISIJ Int*., 41 (2001**)** 590.
5. T. Kushida, H. Matsumoto, N. Kuratomi, T. Tsumura, F. Nakasato and T. Kudo, *Tetsu-to-Hagané*, 82 (1996**)** 37.
6. M. Robinson and P. Kilgallon, *Corros. Sci*., 50 (1994) 626.
7. J. Ćwiek and K. Nikiforov, *Mater. Sci*., 40 (2004) 831.
8. M.S. Han, J.C. Park, S.K. Jang and S.J. Kim, *Phys. Scr.*, T139 (2010) 014037.
9. S. Dey, A.K. Mandhyan, S.K. Sondhi and I. Chattoraj, *Corros. Sci*., 48 (2006) 2676.
10. S.S.M. Tavares, I.N. Bastos, J.M. Pardal, T.R. Montenegro and M.R. Silva, *Int. J. Hydrog. Energy*, 40 (2015**)** 16992.
11. T. Zhang, W. Zhao, T. Li, Y. Zhao, Q. Deng, Y. Wang and W. Jiang, *Corros. Sci*., 131 (2018) 104.
12. M. Nagumo, M. Nakamura and K. Takai, *Metall. Mater. Trans*. *A*, 32 (2001) 339.
13. K. Takai and R. Watanuki, *ISIJ Int*., 43 (2003) 520.
14. M. Wang, E. Akiyama and K. Tsuzaki, *Scr. Mater*., 53 (2005) 713.
15. S. Li, Z. Zhang, E. Akiyama, K. Tsuzaki and B. Zhang, *Corros. Sci*., 52 (2010) 1660.
16. Y. Hagihara, *ISIJ Int*., 52 (2012) 292.
17. A. Nagao, C.D. Smith, M. Dadfarnia, P. Sofronis and I.M. Robertson, *Acta Mater*., 60 (2012) 5182.
18. M. Koyama, E. Akiyama, K. Tsuzaki and D. Raabe, *Acta Mater*., 61 (2013) 4607.
19. A. Turnbull, *Int. J. Hydrog. Energy*, 40 (2015) 16961.
20. M.J. Peet and T. Hojo, *Metall. Mater. Trans*. *A*, 47 (2016) 718.
21. N. Suzuki, N. Ishii, T. Miyagawa and H. Harada, *Tetsu-to-Hagané*, 79 (1993) 227.
22. S. Yamasaki and T. Takahashi, *Tetsu-to-Hagané*, 83 (1997) 454.
23. M. Wang, E. Akiyama and K. Tsuzaki, *Mater. Sci. Eng*. *A*, 398 (2005) 37.
24. M. Wang, E. Akiyama and K. Tsuzaki, *Scr. Mater*., 52 (2005) 403.
25. S. Li, E. Akiyama, K. Yuuji, K. Tsuzaki, N. Uno and B. Zhang, *Sci. Technol. Adv. Mater*., 11 (2010) 025005.
26. K. Hirai, K. Wakiyama and N. Uno, *J. Struct. Constr. Eng*. *AIJ*, 490 (1996) 215.
27. K. Hirai and N. Uno, *J. Struct. Constr. Eng. AIJ*, 560 (2002) 197.
28. Y. Hagihara, C. Ito, N. Hisamori, H. Suziki, K. Takai and E. Akiyama, *Tetsu-to-Hagané*, 94 (2008) 215.
29. Y. Hagihara, C. Ito, D. Kirikae, N. Hisamori, H. Suziki and K. Takai, *Tetsu-to-Hagané*, 95 (2009) 489.
30. Y. Hagihara, *ISIJ Int*., 52 (2012) 292.
31. S. Takagi, Y. Hagihara, T. Hojo, W. Urushihara and K. Kawasaki, *ISIJ Int*., 56 (2016) 685.
32. S. Takagi, S. Terasaki, K. Tsuzaki, T. Inoue and F. Minami, *ISIJ Int*., 45 (2005) 263.
33. S. Li, J. Yin, C. Wang, C. Hou and F. Li, *Int. J. Electrochem. Sc*., 14 (2019) 2705.
34. W.Y. Choo and J.Y. Lee, *Metall. Trans*. *A*, 13 (1982) 135.
35. F.G. Wei, T. Hara and K. Tsuzaki, *Metall. Mater. Trans*. *B*, 35 (2004) 587.
36. C. Wang, H. Qiu, Y. Kimura and T. Inoue, *Mater. Sci. Eng*. *A*, 669 (2016) 48.

37. T. Chida, Y. Hagihara, E. Akiyama, K. Iwanaga, S. Takagi, M. Hayakawa, H. Ohishi, D. Hirakami and T. Tarui, *ISIJ Int*., 56 (2016) 1268.
38. Guidebook for evaluating delayed fracture properties of high strength bolts. *Journal of Steel Structures and Construction Technical Report*, 1 (2010) 38.
39. H. Wagonblast and H.A. Wriedt, *Metall. Trans.*, 2 (1971) 1393.